View metadata, citation and similar papers at core.ac.uk
brought to you by CORE
provided by Tomsk State University Repository

ISSN 0015-4628, Fluid Dynamics, 2015, Vol. 50, No. 1, pp. 79–86. © Pleiades Publishing, Ltd., 2015.
Original Russian Text © V.A. Arkhipov, I.M. Vasenin, A.S. Tkachenko, A.S. Usanina, 2015, published in Izvestiya Rossiiskoi Akademii Nauk, Mekhanika Zhidkosti i Gaza, 2015, Vol. 50, No. 1, pp. 86–94.

Unsteady Rise of a Bubble in a Viscous Fluid at Small Reynolds Numbers

V. A. Arkhipov[a], I. M. Vasenin[a], A. S. Tkachenko[b], and A. S. Usanina[a]

[a]*Tomsk State University, Faculty of Physics and Engineering, pr. Lenina 36, Tomsk, 634050 Russia*

[b]*Tomsk State Pedagogical University, Faculty of Technology and Entrepreneurship, ul. Karla Ilmera 15/1, Tomsk, 634057 Russia*

e-mail: leva@niipmm.tsu.ru

Received May 20, 2014

Abstract—A bubble rising from the state of rest in a viscous incompressible fluid is considered. A formula for the Basset force acting on the bubble in a viscous fluid is obtained, which differs by a multiplier from the Basset force for a solid particle. The problem of unsteady rise of a bubble is solved analytically. The bubble rise is also studied experimentally and the experimental data are compared with the theoretical results.

Keywords: bubble, viscous fluid, unsteady regime, Basset force.

DOI: 10.1134/S0015462815010093

Investigation of the laws of bubble motion in a fluid is a classical problem of hydrodynamics. The interest in the dynamics of bubbles is attributable to their role in a number of practical problems, connected with two-phase flows in power plants, heat transfer in boiling, cavitation, underwater acoustics, flotation, cooling of nuclear reactors, and other physical processes. In the problems listed above, a significant factor is the variation of the bubble velocity in the fluid.

An analysis of the literature indicated that only a limited number of studies is devoted to unsteady motion of a single bubble. In most experiments, a steady rise of a single bubble (the drag law, the loss of stability of the bubble shape) or a high-concentration system of bubbles are considered. The theoretical analysis of unsteady motion of dispersed inclusions was performed mainly for solid spherical particles [1, 2]. In [1], the results of experimental study are also presented.

Among the experimental studies of single-bubble motion with account of unsteady and "memory" effects, the papers [3] and [4] should be noted. In [3], using the dimension analysis for Reynolds numbers Re ranging between 0.01 and 100, an empirical dependence of the bubble drag coefficient on Re was obtained with account for the unsteady and "memory" forces. However, the results obtained cannot be used for practical calculations due to indeterminacy of some parameters entering in this dependence. The analysis of experimental results [4] for the velocity of unsteady rise of a bubble is impossible because the authors did not specify the values of physical parameters of the fluid.

Among the theoretical studies of unsteady motion of a bubble in a viscous fluid, we note papers [5–8]. The motion of a solid, liquid, and gaseous spherical inclusion was investigated on the basis of an approximate solution of the linearized Navier–Stokes equations by an operational method. The main result of [5–8] is the conclusion that, for a solid particle and a gas bubble of the same size, the dimensionless velocities u/u_∞ are close to each other.

A detailed review of the theoretical and experimental results on the unsteady rise of a bubble is given in [9]. The aim of the present study is an experimental and theoretical analysis of the rise of a single bubble in a viscous fluid.

1. THEORETICAL ANALYSIS

We will consider only a translational motion of the bubble center and estimate the drag force F_C exerted on the bubble in its unsteady motion in a viscous fluid. We will use the approach similar to [10], applied earlier for determining F_C of a solid sphere.

As in [10], we will study the fluid flow at small Reynolds numbers, assuming that the bubble shape is spherical. The only difference is in the boundary condition. For a solid sphere, the no-slip conditions are specified, while for a bubble occupied by a low-viscosity gas, we will use the no-flow condition and the absence of a shear stress on the bubble surface.

At first, we will calculate the drag force exerted on a bubble of radius R, when it oscillates harmonically with the velocity $\mathbf{u} = \mathbf{u}_m \exp(-i\omega t)$, where $\mathbf{u}_m$ is the oscillation amplitude, ω is the oscillation frequency, and t is the time. As in [10], the fluid velocity is sought in the form

$$\mathbf{V} = \exp(-i\omega t)\,\mathrm{curl}\,\mathrm{curl}(f(r)\mathbf{u}_m). \tag{1.1}$$

We substitute (1.1) in the equation

$$\frac{\partial}{\partial t}\mathrm{curl}\,\mathbf{V} = \nu\Delta\,\mathrm{curl}\,\mathbf{V}.$$

Here, ν is the kinematic viscosity of the fluid. For the function $f(r)$, we obtain the equation

$$\Delta^2 f + \frac{i\omega}{\nu}\Delta f = 0. \tag{1.2}$$

After the integration of (1.2), we obtain:

$$f' = a\frac{\exp(icr)}{r^2}\left(r - \frac{1}{ic}\right) + \frac{b}{r^2}. \tag{1.3}$$

Here, a and b are the integration constants. Since $ic = -(1-i)\sqrt{\omega/2\nu}$, the right-hand side of Eq. (1.2) tends to zero, as $r \to \infty$. In the spherical coordinates, with account of (1.1) the components of velocity $\mathbf{V}$ can be written as follows:

$$V_r = \exp(-i\omega t)(\mathrm{curl}\,\mathrm{curl}\,f\mathbf{u}_m)_r = 2\exp(-i\omega t)u_m\cos\theta\frac{f'}{r}, \tag{1.4}$$

$$V_\theta = \exp(-i\omega t)(\mathrm{curl}\,\mathrm{curl}\,f\mathbf{u}_m)_\theta = \exp(i\omega t)\left(\frac{ica\exp(icr)}{r} - \frac{f'}{r}\right)u_m\sin\theta, \tag{1.5}$$

where θ is the polar angle, measured from the bubble velocity direction.

Since on the bubble surface the radial velocity of the fluid is equal to the velocity of the surface points in the radial direction r, then for the radial velocity at $r = R$ from (1.4) we obtain:

$$\frac{f'(R)}{R} = -\frac{1}{2}. \tag{1.6}$$

With account of (1.6), the condition of the absence of shear stresses on the bubble surface

$$\left(\frac{1}{r}\frac{\partial V_r}{\partial\theta} + \frac{\partial V_\theta}{\partial r} - \frac{V_\theta}{r}\right)_{r=R} = 0$$

takes the form

$$\frac{3}{R} + \left(\frac{3}{R} - ic\right)\frac{ica\exp(icR)}{R} = 0.$$

There follows:

$$\frac{ica\exp(icR)}{R} = -\frac{1}{1 - icR/3} = -\frac{1}{1 - (i - 1)Rq/3}.$$

where $q = \sqrt{\omega/2\nu}$.

For limited valued of ω and small R, such that $(R/3)\sqrt{\omega/2\nu} \ll 1$, we neglect the quantity $(1 - i)(R/3)\sqrt{\omega/2\nu}$ in the denominator, as compared to unity, and assume that

$$\frac{ica\exp(icR)}{R} = -1. \tag{1.7}$$

The projection of the bubble drag F_C on the direction of $\mathbf{u}_m$ is calculated using the formula

$$F_C = \int_0^\pi \left(-P\cos\theta + 2\mu\frac{\partial V_r}{\partial r}\cos\theta \right) 2\pi R^2 \sin\theta\, d\theta, \tag{1.8}$$

where P is the pressure and μ is the dynamic viscosity of the fluid. Here, we take into account that the shear stress on the bubble surface vanishes.

The pressure distribution at $r = R$ is found by the integration of the projection of the fluid motion equation on the θ-direction over θ at $r = R$:

$$\frac{\partial V_\theta}{\partial r} = -\frac{1}{\rho R}\frac{\partial P}{\partial \theta} + \nu\left(\Delta V_\theta + \frac{2}{R^2}\frac{\partial V_r}{\partial \theta} - \frac{V_\theta}{R^2\sin^2\theta} \right), \tag{1.9}$$

where ρ is the fluid density. After the substitution of the velocity in (1.9) with account of (1.6) and (1.7) and the integration over θ we obtain:

$$P = P_0\exp(-i\omega t) + \nu\rho\cos\theta u_m \exp(-i\omega t)\left(\frac{1}{R} - ic + R(ic)^2 - \frac{i\omega\rho R}{2\mu} \right). \tag{1.10}$$

Since the integral (1.8) of the constant P_0 is zero, this constant was not calculated.

After the substitution of the pressure P and the derivative $\partial V_r/\partial r$ in Eq. (1.8), we obtain the expression for the drag of a bubble, oscillating harmonically with the velocity $\mathbf{u}_m\exp(-i\omega t)$:

$$F_c = -\pi\rho R^2 u_m \exp(-i\omega t)\left[\frac{4\nu}{R} - \frac{2}{3}i\omega t + \frac{2}{3}(1 - i)\frac{\sqrt{2\nu}}{R}\sqrt{\omega} \right], \tag{1.11}$$

where the sign "$-$" indicates the direction of the drag force, opposite to the bubble velocity.

We will now calculate the drag force of a bubble moving with an arbitrary velocity $u(t)$. We represent the bubble velocity as a Fourier integral

$$u(t) = \frac{1}{2\pi}\int_{-\infty}^{\infty} u_\omega \exp(-i\omega t)\, d\omega, \tag{1.12}$$

where

$$u_\omega = \int_{-\infty}^{\infty} u(\tau)\exp(i\omega\tau)\, d\tau.$$

In this case, the drag force is represented as the integral of the drag forces for the motions with the velocities equal to the Fourier components $u_\omega\exp(-i\omega t)$. These forces are calculated using formula (1.12), which with account of the equality $(du/dt)_\omega = -i\omega u_\omega$ takes the form:

$$-\pi\rho R^3\exp(-\omega t)\left(\frac{4\nu}{R^2}u_\omega + \frac{2}{3}\left(\frac{du}{dt}\right)_\omega + \frac{2}{3}\frac{\sqrt{2\nu}}{R}\frac{(1 + i)}{\sqrt{\omega}} \right). \tag{1.13}$$

Relations (1.13) differ from the similar formula for the solid sphere [10] only by the multipliers in the first and third terms. Accordingly, the Fourier integral differs from the analogous integral only by these coefficients. Repeating the calculations performed in [10], we obtain

$$F_C = -2\pi\rho R^3\left(\frac{1}{3}\frac{du}{dt} + \frac{2\nu}{R^2}u + \frac{2}{3}R\sqrt{\frac{\nu}{\pi}}\int\limits_{-\infty}^{t}\frac{du}{d\tau}\frac{d\tau}{\sqrt{t-\tau}}\right). \tag{1.14}$$

The first term in expression (1.14) describes the force attributable to the added mass of the sphere in a potential flow. The second term gives the contribution to the viscous drag in accordance with the Hadamard–Rybcziski formula for a bubble. The third term describes the Basset force, which for a bubble is 9/2-fold smaller than for a solid sphere.

We will now consider a model of bubble rise in an unbounded viscous fluid. With account of the gravity force, the Archimedes force, and the drag force, the equation of bubble motion takes the form:

$$V_p\rho_p\frac{du}{dt} = -\frac{1}{2}V_p\rho\frac{du}{dt} - 4\pi\mu Ru - V_p(\rho_p - \rho)g - \frac{4}{3}\pi R^2\sqrt{\frac{\nu}{\pi}}\int\limits_{-\infty}^{t}\frac{du}{d\tau}\frac{d\tau}{\sqrt{t-\tau}}, \tag{1.15}$$

where V_p is the bubble volume, ρ_p is the gas density, and g is the gravity force acceleration. Since $\rho_p \ll \rho$, we neglect the terms with ρ_p in (1.15).

Introducing the characteristic time scale $T_0 = \rho R^2/6\mu$ and the dimensionless time $\bar{t} = t/T_0$, we rewrite Eq. (1.15) in the form:

$$\frac{du}{d\bar{\tau}} + u + \sqrt{\frac{2}{3\pi}}\int\limits_{-\infty}^{\bar{t}}\frac{du}{d\bar{t}}\frac{d\bar{\tau}}{\sqrt{\bar{t}-\bar{\tau}}} = 2gT_0. \tag{1.16}$$

Using conditions $u(0) = 0$ and $du/d\bar{\tau} = 0$ for $\bar{\tau} < 0$, we represent Eq. (1.16) in the form

$$\frac{du}{d\bar{t}} + \int\limits_{0}^{\bar{t}}\frac{du}{d\bar{\tau}}d\bar{\tau} + \sqrt{23\pi}\int\limits_{0}^{\bar{t}}\frac{du}{d\bar{\tau}}\frac{d\bar{\tau}}{\sqrt{\bar{t}-\bar{\tau}}} = 2gT_0.$$

Introducing the acceleration $a = du/d\bar{t}$, we can write

$$a + \int\limits_{0}^{\bar{t}} a\,dt + \sqrt{23\pi}\int\limits_{-\infty}^{\bar{t}} a\frac{d\bar{\tau}}{\sqrt{\bar{t}-\bar{\tau}}} = 2gT_0.$$

This equation has an exact solution

$$a(\bar{t}) = \frac{4}{\sqrt{\pi}}gT_0\int\limits_{0}^{\infty}\exp\left(-\sqrt{\frac{2}{3}}\bar{t}x\right)\left(\cos\sqrt{\frac{10}{3}}\bar{t}x - \frac{1}{\sqrt{5}}\sin\sqrt{\frac{10}{3}}\bar{t}x\right)\exp(-x^2)\,dx,$$

which is obtained using the operational Laplace transform method [11].

When the acceleration is found, the velocity is calculated as

$$u(\bar{t}) = \int\limits_{0}^{\bar{t}} a\bar{t}\,d\bar{t}.$$

2. EXPERIMENTAL STUDY

The experiments were performed with a set-up, which consisted of a transparent cavity with plane-parallel walls, filled with a working fluid, a facility for bubble generation, and a system of visualization of the single-bubble rise (Fig. 1).

The cavity, made from an optic glass 5 mm thick, had a prismatic shape, measured $150 \times 150 \times 600$ mm. To vary the bubble size, we used needles with different outlet diameters, placed in the base of the cavity.

The visualization system included the light sources (luminescent lamps of power 18 W), mounted on the back panel throughout the entire height of the cavity, a Panasonic HDC-SD60 digital video camera, and two Citius C100 high-speed video cameras. Video filming of the process under study at different angles made it possible to increase the accuracy and to ensure the control of variation of the bubble rise parameters in different stages of bubble motion. The first camera recorded the bubble dynamics in the initial unsteady stage of motion, the second recorded the bubble motion on the entire trajectory. The videofilming was performed with the 1280×670 resolution, speed of 700 frames/s, and exposure time of 1/500–1/2000 s. The third camera was used for measuring the bubble size; the exposure area was 5×5 cm with 2-fold zoom.

To increase the accuracy of the experimental data, in this study we used a liquid with stable physico-chemical properties in the range of working temperatures 17–22°C, namely, a solution of a castor oil in alcohol.

In the experiments, we determined the following parameters: the dynamic viscosity coefficient μ_l, the solution density ρ_l, the bubble diameter D, and the bubble rising velocity u. Using the experimentally measured parameters, we calculated the values of the Reynolds number Re and the drag coefficient C. The density of the liquid was measured by an areometer ($\rho_l = 935$–960 kg/m^3). The solution viscosity $\mu_l = 0.23$–1.13 Pa$\times s$ was estimated using the Stokes formula for gravitational settling of a solid particle. The bubble diameter $D = 3.2$–5.5 mm was determined from the processing of the photographs. The path and the velocity of the bubble were determined from a frame-by-frame processing of the results of high-speed videofilming. The velocity of the bubble rise at a certain height h_i was calculated using the formula

$$u(h_i) = \frac{h_{i+1} - h_{i-1}}{\Delta t_i} \qquad (i = 1,\ 2, \ldots,\ N),$$

where h_{i-1}, h_{i+1} are the paths covered by the bubble on the $i - 1$-th and $i + 1$-th frames, respectively; Δ_i is the time interval between the $i - 1$-th and $i + 1$-th frames, and N is the number of the frames.

The equation of bubble motion contains the viscous drag law. For small $\mathrm{Re} < 1$, the drag force coefficient of a spherical inclusion is given by the Hadamard–Rybczinski formula

$$C = \frac{24}{\mathrm{Re}}\left(\frac{3\mu_* + 2}{3 + 3\mu_*}\right), \qquad \mathrm{Re} = \frac{\rho_l u D}{\mu_l}. \tag{2.1}$$

Here, $\mu_* = \mu/\mu_l$ is the ratio of the dynamic viscosities of the dispersed μ and carrier μ_l phase. In the limiting cases, from (2.1) the drag force coefficient takes the form

$$C = \frac{A}{\mathrm{Re}}, \tag{2.2}$$

where $A = 16$ for a bubble ($\mu_* \to 0$) and $A = 24$ for a solid sphere ($\mu_* \to \infty$).

To refine the drag force coefficient, we performed a series of experiments in a steady-state regime. The results are given in Table 1: experimental values of the steady-state bubble rise velocity u_e, Reynolds number Re, and the drag force coefficient C_e. In calculating the Reynolds number, we used the experimental data for the steady-state bubble rise velocity, the bubble size, and the physical properties of the fluid. The value of the experimental drag force coefficient C_e was determined from the bubble motion equation for the steady-state regime using the formula

$$C_e = \frac{4}{3} g(\rho_l - \rho)\frac{D}{\rho_l u_e^2}.$$

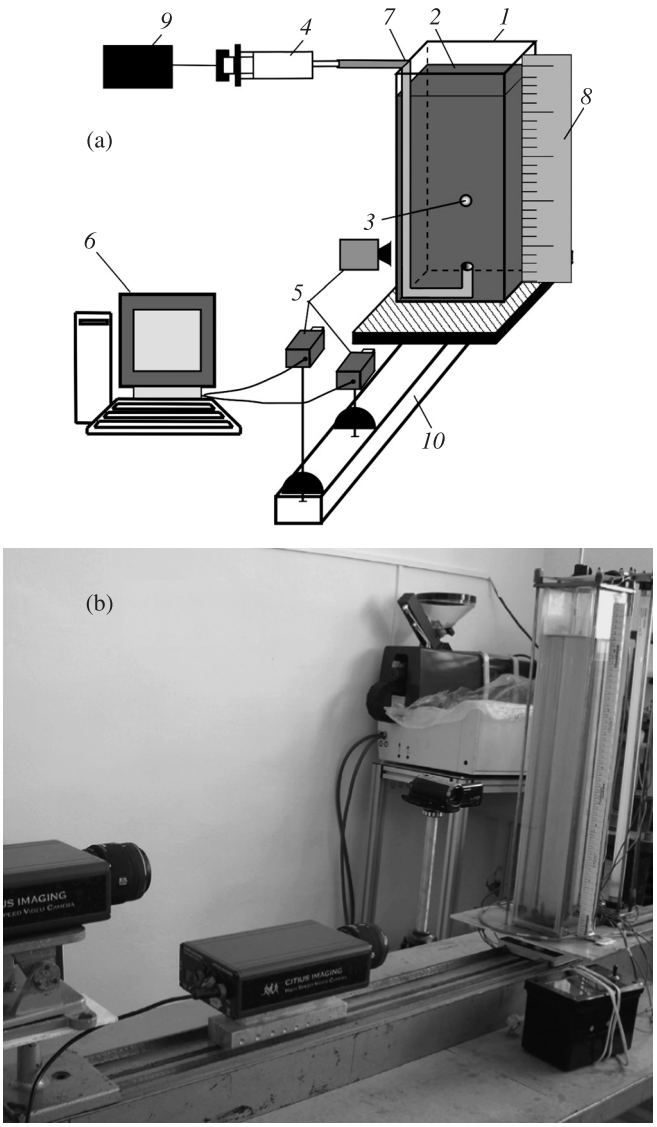

Fig. 1. Scheme (a) and photograph (b) of the experimental set-up: (*1*) cavity; (*2*) working fluid; (*3*) bubble; (*4*) bubble generator; (*5*) video cameras; (*6*) computer; (*7*) tube; (*8*) measuring rule; (*9*) electric motor; (*10*) optic bench.

The relative error in determining C_e was calculated using the formula

$$\delta C_e = \delta D + 2\delta u_e, \tag{2.3}$$

where $\delta D = 3\%$ and $\delta u_e = 0.1\%$. In the estimates of δC_e, we neglect the errors in the measurement of ρ and ρ_l due to their smallness. For our experimental conditions, the errors of the experimental determination of the drag force coefficient did not exceed 3%. By analogy with (2.2), the dependence $C_e(\mathrm{Re})$ was approximated by the formula

$$C_e = \frac{15.5}{\mathrm{Re}}. \tag{2.4}$$

The values of the drag force coefficients calculated using formula (2.2) for $A = 16$ and $A = 15.5$ are given in table. In Fig. 2, we have plotted both the calculated and experimental values of the drag force coefficient the Reynolds number ranging between 0.03 and 0.55. The minimal difference between the theoretical and experimental value of C_e is observed for dependence (2.3) with a mean-square deviation $\delta = 1.9\%$. For the Hadamard–Rybcziski dependence ($A = 16$), the deviation is $\delta = 2.2\%$. The Stokes expression for the drag force coefficient ($A = 24$) gives the results which differ significantly from the experimental data (Fig. 2).

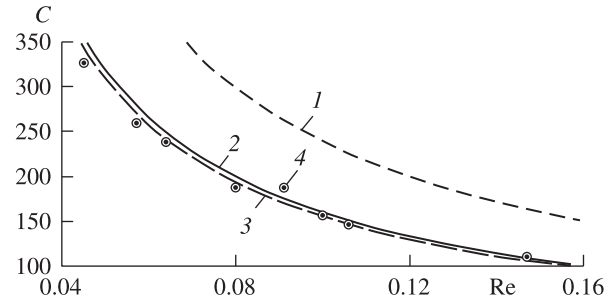

Fig. 2. Drag force coefficient as a function of the Reynolds number: (*1–3*) $A = 24$, 16, 15.5; (*4*) experimental values of C_e.

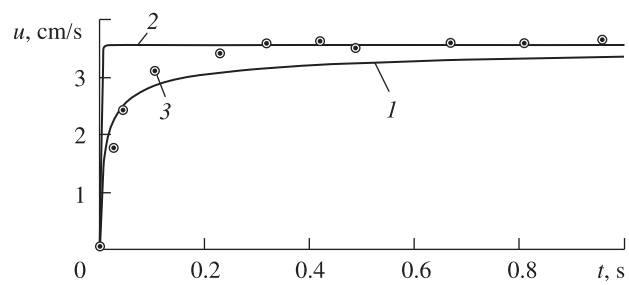

Fig. 3. Time dependence of the bubble rise velocity with (*1*) and without (*2*) taking the Basset force into account; (*3*) experimental data.

Experimental results for steady-state bubble rise

D, mm	ρ_l, kg/m^3	μ_l, Pa s	u_e, cm/s	Re	$A = 16$	$A = 15.5$	C_e
3.7	960	1.13	0.88	0.028	571.4	553.6	624
3.6	960	0.92	1.2	0.045	355.5	344.4	326
3.9	960	0.92	1.4	0.057	280.7	271.9	260
4.1	960	0.92	1.5	0.064	250.0	242.2	238
4.4	960	0.92	1.75	0.08	200.0	193.7	188
5.5	960	1.13	1.96	0.091	175.8	170.3	187
4.8	960	0.92	2.0	0.1	160.0	155	157
4.9	960	0.92	2.09	0.106	150.9	146.2	146
5.5	960	0.92	2.55	0.146	109.6	106.2	110
3.2	935	0.23	3.6	0.47	34.0	32.9	28.9
3.4	935	0.23	4.0	0.56	28.6	27.7	27.7

3. A COMPARATIVE ANALYSIS OF THE RESULTS

Figure 3 shows the time dependence of the bubble rise velocity obtained from the solution of bubble motion equation (1.15) with account of all force components (curve *1*). The calculations were performed for the experimental parameters given above. The value of the constant in the viscous drag law was taken from the experiment $A = 15.5$. We also plot the dependence $u(t)$, in which the added mass force is taken into account, but the Basset force is neglected (curve *2*).

An analysis of the data given in Fig. 3 shows that the dependence $u(t)$ obtained without the Basset force does not reflect the real dynamics of the bubble rise on the unsteady interval of its trajectory but describes adequately the steady-state regime.

The dependence $u(t)$, calculated with account of the Basset force, agrees satisfactorily with the experimental data on the initial interval of the bubble trajectory (the difference does not exceed 5%). The calculated dependences $u(t)$ are characterized by a slow transition to the steady-state regime. For $t > t_* = 0.15$ s, the difference between the calculated and experimental bubble velocity is within 9%. We note that the similar "long" transition of the particle velocity to the steady-state regime was obtained in the theoretical studies of unsteady motion of a dispersed particle [3, 13]. The discrepancy between the calculated and experimental data on the bubble dynamics is attributable, apparently, to an inexact fulfillment of the condition $u = 0$ at $t = 0$ in the experiments.

Summary. The results of theoretical study of unsteady rise of a bubble in a viscous fluid at small Reynolds numbers indicated that the unsteady Basset force affects significantly the laws of the bubble rise.

A comparison of the theoretical and experimental data for the bubble rise velocity on the unsteady interval demonstrated a satisfactory agreement of the results.

The work received financial support from the RF President grant (MK-1259.2013.1) and the RF Ministry of Science and Education in the framework of State Program No. 2014/223 (code 1567).

REFERENCES

1. I.S. Vodop'yanov, A.G. Petrov, and M.M. Shunderyuk, "Unsteady Sedimentation of a Spherical Particle in a Viscous Fluid," Fluid Dynamics **45** (2), 254–263 (2010).
2. E.V. Visitskii, A.G. Petrov, and M.M. Shunderyuk, "The Motion of a Particle in a Viscous Fluid under Gravity, Vibration and Basset's Force," J. Appl. Math. Mekh. **73** (5), 548–557 (2009).
3. Li Zhang, Chao Yang, Zai-Sha Mao, "Unsteady Motion of a Bubble in Highly Viscous Solution and Empirical Correlation of Drag Coefficient," Chem. Eng. Sci. (63), 2099–2106 (2008).
4. W.C. Park, J.F. Klausner, and R. Mei, "Unsteady Forces on Spherical Bubbles," Exp. Fluids (19), 167–172 (1995).
5. A.S. Sangani, D.Z. Zhang, and A. Prosperetti, "The Added Mass, Basset, and Viscous Drag Coefficients in Nondilute Bubbly Liquids Undergoing Small-Amplitude Oscillatory Motion," Phys. Fluids **A3** (12), 2955–2970 (1991).
6. R. Mei and J.F. Klausner, "Unsteady Force on a Spherical Bubble at Finite Reynolds Number with Small Fluctuations in the Free-Stream Velocity," Phys. Fluids A **4** (1) 63–70 (1992).
7. M. Parmar, S. Balachandar, and A. Haselbacher, "Equation of Motion for a Drop or Bubble in Viscous Compressible Flows," Phys. Fluids **24**, 056103 (2012).
8. B.I. Bronshtein and G.A. Fishbein, *Hydrodynamics, Mass, and Heat Transfer in Disperse Systems* [in Russian] (Khimiya, Leningrad, 1977).
9. R. Clift, J.R. Grase, and M.H. Weber, *Bubbles, Drops, and Particles* (Acad. Press, New York, 1978).
10. L.D. Landau and E.M. Lifshits, *Fluid Mechanics* (Pergamon Press, Oxford, 1975).
11. M.A. Lavrent'ev and B.V. Shabat, *Methods of Theory of Complex-Variable Functions* [in Russian] (Nauka, Moscow, 1987).
12. V.A. Arkhipov, I.M. Vasenin, and A.S. Usanina, "Experimental Study of Unsteady Regimes of Single-Bubble Rise," Inzh. Fiz. Zh. **86** (5), 1097–1106 (2013).
13. A.J. Dorgan and E. Loth, "Efficient Calculation of the History Force at Finite Reynolds Numbers," Int. J. Multiphase Flow **33**, 833–848 (2007).